ASIAN JOURNAL OF CIVIL ENGINEERING (BUILDING AND HOUSING) VOL. 8, NO. 6 (2007)
PAGES 581-595

A NEW METHOD FOR IMPROVING DUCTILITY IN EXISTING RC ORDINARY MOMENT RESISTING FRAMES USING FRPS

S.S. Mahini* and H.R. Ronagh
[a]Department of Civil Engineering, Yazd University, Yazd, Iran
[b]Division of Civil Engineering, School of Engineering, The University of Queensland, Brisbane, QLD 4072, Australia

ABSTRACT

In the recent years, attempts have been made to upgrade existing RC Ordinary Moment Resisting Frames (OMRF) into Ductile Moment Resisting Frame (DMRF). In practice, this can be implemented by controlling the plastic hinges locations. This paper presents the results of an experimental study performed to evaluate the ability of CFRP sheets in preventing the plastic hinge formation at the face of the column in exterior RC joints. Five plain/CFRP-retrofitted scaled-down joints of a typical OMRF were tested under monotonic/cyclic loads to failure. The results show that carbon fibre can effectively relocate the plastic hinge away from the column face.

Keywords: Carbon fibre sheets, reinforced concrete joints, plastic hinge

1. INTRODUCTION

In designing an ordinary moment resisting frame, often the principle of *strong-column-weak beam* is implemented in order to make sure that plastic hinging occurs in the beams and as such the frame is capable of dissipating significant energy while remaining stable in the inelastic region. The stability in this context is defined as the ability of the frame to maintain it's elastic level of resistance throughout the entire inelastic range of response. Using this principle, plastic hinges would develop in the beams adjacent to the joints and usually very close to the column face. The problem is that this closeness may allow cracks caused by plastic hinging to propagate into the joint core region and as such initiate a brittle failure mechanism.

Attempts have been made in the past in order to develop methods of relocating a plastic hinge away from the column face. Most of the methods, however, have been on detailing of reinforcing bars, which can only be utilised in new construction. For example, Abdel-Fattah and Wight [1] showed that the use of intermediate longitudinal beam reinforcement combined with extra top and bottom steel in the beam at a specific length can help in

* Email-address of the corresponding author: s.mahini@yazduni.ac.ir

successfully relocating a plastic hinge away from the column face. The relocating was also studied by Joh et al. [2]. Four half-scale RC interior beam-column joints with different reinforcement details in the beam in the region adjacent to the column were tested under cyclic loads in their investigation. Their results showed that the bond deterioration within the joint may be prevented by the relocation of plastic hinge, while shear sliding may occur at the plastic hinge zone due to the increased shear force at the beam end. (Joh et al. [2]) proposed a new arrangement for the beam bars in order to improve the plastic hinging. Paulay and Priestley [3] also proposed that the beam bars may be curtailed so that stresses in the reinforcement would not exceed yield stress at the face of the column, while strain hardening may be developed at the critical section of the plastic hinge. Paulay and Priestley [3] concluded that the critical section must be a sufficient distance away from the column face. They recommended that because the nature of shear transfer across the critical section of a plastic hinge is complicated, care must be taken with detailing of the shear reinforcement. Paulay and Priestley [3] proposed that this necessitates stirrups extending between these two regions, perhaps supplemented by specially bent top beam bars, to carry the entire shear force and also suggested that to ensure that the critical section occurs at a chosen place, extra flexural reinforcement can be provided by bending some of the top and bottom bars at an angle of 45° or less into the opposite face of the beam.

Many already existing moment resisting frames do not possess correct joint reinforcement detailing as they have been designed based on older codes. A different method which can upgrade the joints of these frames in an efficient and cost effective way is consequently desirable. This paper presents results of an experimental investigation into the effectiveness of FRP wraps in controlling the location of a plastic hinge in an Ordinary Moment Resisting Frame (OMRF). The proposed method is to stick carbon FRP sheets of specific lengths to the sides of the beams of a reinforced concrete joint (i.e. web-bonded FRP) and extend them over the joint to act as an anchor. The performance of this method has been investigated by the authors and is presented in the following. Other aspects of the investigation can be found in papers [4, 5]. The method can be used just as effectively for the repair of earthquake damaged RC exterior joints.

2. POTENTIAL PLASTIC HINGE ZONES

Designing beam column joints is considered to be a complex and challenging task for structural engineers and careful design of joints in RC frame structures is crucial to the safety of the structure. Although the sizing of the joint is determined by the size of the frame members, joints are subjected to a different set of loads from those used in designing beams and columns. As a result, it is necessary to pay special attention to the ductility of the reinforcement within the joint region. If the joint is not designed properly, the possibility of plastic hinge formation in the columns increases substantially. This is dangerous for two reasons; firstly the collapse mechanism associated with hinges in the columns has a lower ultimate load and secondly the energy absorbance of plastic hinges within the columns is normally less due to reinforcement arrangement and the axial load as is seen in Figure 1. Engineers can avoid this when designing Ductile Moment Resisting Frames (DMRFs) by

employing the principle of *strong-column weak-beam* design. According to this design principle, joints are designed in such a way that the joint region and the column remain essentially elastic under the action of high lateral loads such as earthquake and high-pressure winds while the main energy dissipation occurs within the plastic hinges formed in the beams.

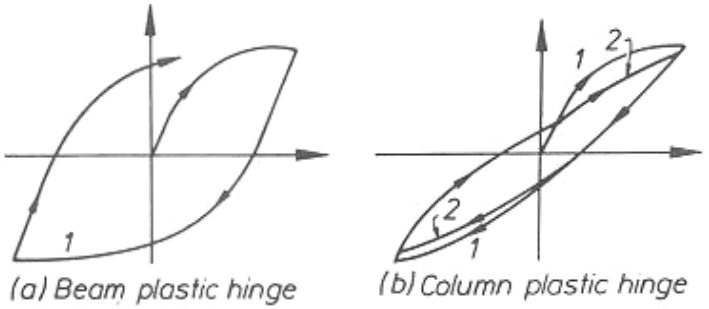

Figure 1. Typical measured lateral-load displacement hysteresis loops for subassemblies of structural concrete [3]

One of the determining factors to ensure a weak beam in a DMRF structure is M_R, the ratio of column-to-beam flexural capacity given by,

$$M_R = \frac{\sum M_C}{\sum M_B} \tag{1}$$

Where $\sum M_C$ and $\sum M_B$ are respectively the sum of the flexural capacities of the columns and beams intersecting at the joint. Experimental results indicate that in order to avoid the formation of a plastic hinge in the joint, M_R should be a minimum of 1.4 [6]. Iranian Concrete Code ABA [7] and Australian standard AS3600 [8] prescribes 1.2 and 1.5 respectively for this ratio. In addition to choosing appropriate M_R, care should be taken in making sure that plastic hinges within the beam are sufficiently distanced away from the joint as shown in Figure 2. This is to ensure that penetration of plasticity to the joint core would not occur.

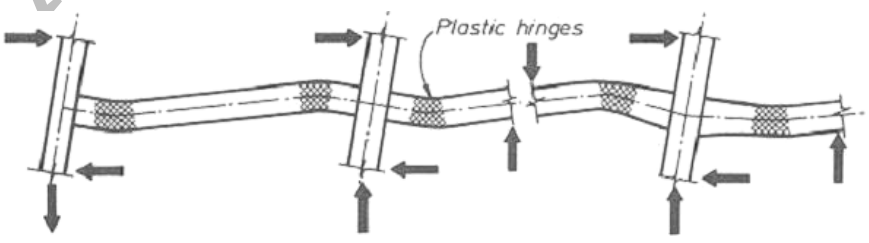

Figure 2. Correct positions of plastic hinges [3]

There are several methods to achieve this. One possibility is to detail the reinforcement as is shown in Figure 3 (a). In this way stresses in the reinforcement do not exceed the yield stress at the face of the column, while strain hardening develops at the critical section of the plastic hinge. A minimum distance equal to beam hight, h_b, or 500 mm, whichever is less, is recommended [3]. Because the nature of shear transfer across the critical section of a plastic hinge is complicated, care must be taken with detailing of the shear reinforcement. As Figure 3 (b) indicates, the beam's shear force V_b introduced to region A by the diagonal forces has to be transferred to the top of the beam in region B. This necessitates stirrups extending between these two regions, perhaps supplemented by specially bent top beam bars, to carry the entire shear force.

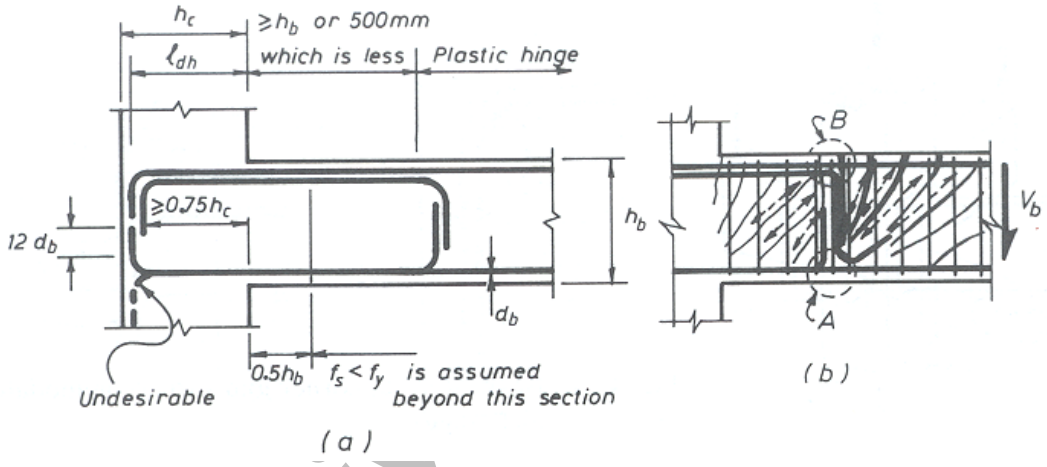

Figure 3. Potential plastic hinge relocated from the face of a column [3]

The method of relocation attempted in the current investigation is different to the mentioned methods and as such is innovative. Here an attempt is made to make use of external FRP warps to strengthen the beam adjacent to the joint and as such to relocate the plastic hinge. The method will be explained in the following section.

3. EXPERIMENTAL PROGRAM

3.1 Selection of Specimen for Test

Figure 4 shows a 1/2.2 scale of the selected frame. This scale was chosen as it allows the similitude requirements to be fulfilled as well as the model to fit in the testing frame. The member section sizes and reinforcement that were obtained based on this scale, satisfied the limitation of the hydraulic actuator size and the ultimate capacity of the hydraulic jacks. The prototype structure is a typical eight story residential RC building located in Brisbane, Australia. The controlling design criterion for this structure is the strength required to resist the applied gravity and lateral loads. The prototype was designed as an Ordinary Moment

Resisting Frame (OMRF), according to the Australian Concrete Code AS3600 [8] with details similar to non-ductile RC frames designed to ACI-318 [9]. A scaled-down frame was modelled by the application of the similitude requirements that relate the model to the prototype using the Buckingham theorem [10]. The scaled-down joints were extended to the column mid-hight and beam mid-span, corresponding to the inflection points of the bending moment diagram under lateral loading.

The scale down frame was loaded, analysed and designed according to AS3600. Four N12 rebars (ϕ12 mm) were used for both the column vertical reinforcement and the beam longitudinal reinforcement. R6.5 bars (ϕ 6.5 mm) were used for stirrups at a spacing of 150 mm in both beam and column. A 30 mm concrete cover was considered for the beam and column reinforcements which is about half of the corresponding cover in prototype. Joint details were designed according to AS3600. For specimens that were tested under cyclic loads, the bottom beam reinforcements should be bent toward the joint core similar to the top beam bars; instead, in order to facilitate caging within the joint core, U-bars were used for beam reinforcements.

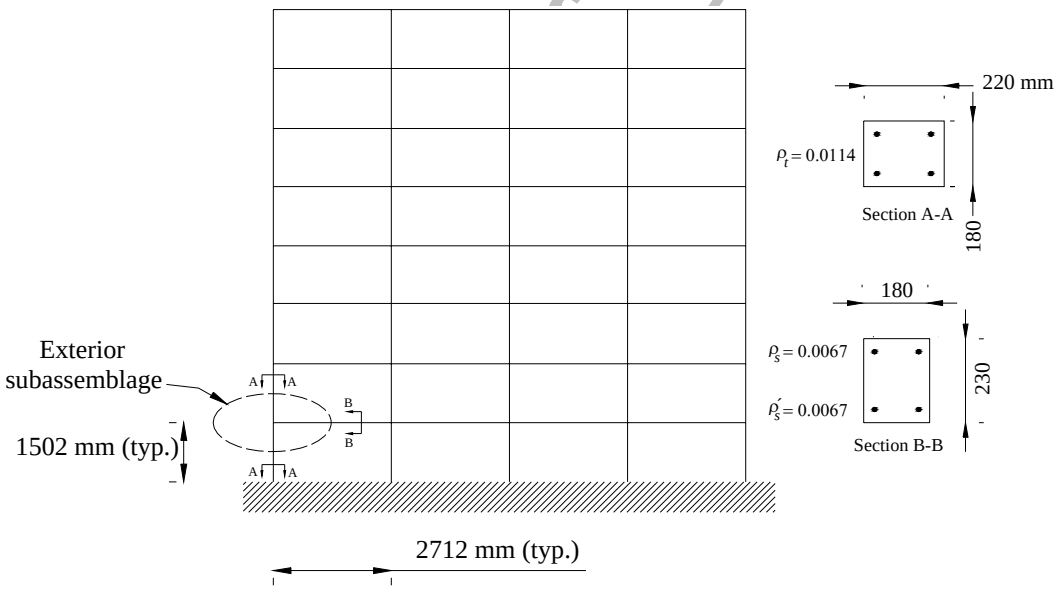

Figure 4. Scale down model of the selected frame.

An exterior beam-column sub-assembly was isolated at the first floor level of the scaled down frame as shown in Figure 4. Although the location of the points of contraflexure of the columns above and below a given story may vary when the frame is subjected to cyclic actions such as earthquake, a good estimate for the mean column shear force can be obtained if it is assumed that the points of contraflexure in all columns provided in a given storey occur approximately at mid-height. Figure 5 shows the deformed shape of a typical story of the selected frame. In this Figure, l is the span length and l_c is the story height. As is seen, the lateral load on this frame produces an interstorey drift of ΔH.

A free body diagram of the selected joint in its deformed position is shown in Figure 6(a). For the testing, however, it was easier to maintain the column in a vertical position as shown in Figure 6(b). In these figures, l_c is the story height, l_b is half beam span corresponding to the length of the beam connected to the selected joint, N is the internal axial force of the column, P is the beam-tip load corresponding to the beam shear force V_b, V_{col} is the column shear force, ΔH is the interstory drift and Δ is the vertical beam-tip displacement.

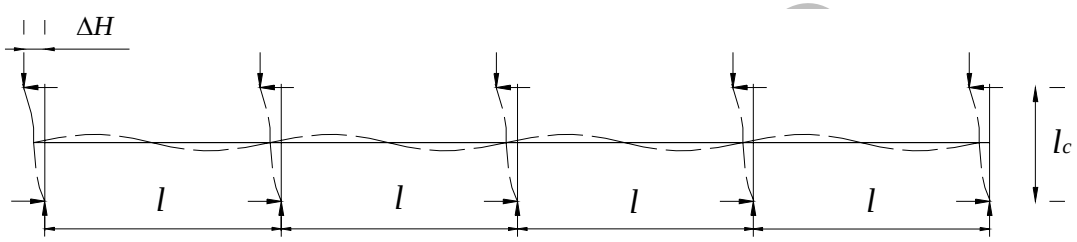

Figure 5. Deformed shape of a story under lateral force

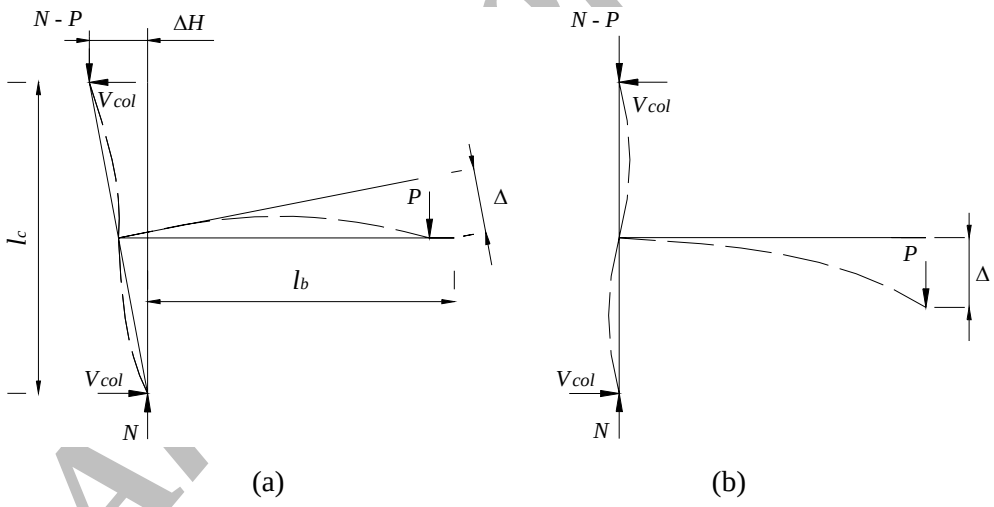

Figure 6. Isolated beam-column test subassembly subjected to lateral loading.

3.2 Description of specimens

The experimental program consisted of testing five 1/2.2 scale exterior RC beam-column joints. Figure 7 summarizes all the test specimens' details. All joints consisted of 180 mm wide and 230 mm deep beams with 220 mm × 180 mm columns. All beams were reinforced with 12 mm diameter (N12) high-strength longitudinal reinforcing steel bars, namely two bars in the top and two bars in the bottom of the beam. Yield strength of the main steel reinforcements, N12 was around 500 MPa and the modulus of elasticity was equal to 200 GPa. All columns were reinforced with fours N12 reinforcing bars, with one bar positioned

at each corner of the columns. The beam stirrups and column ties were 6.5 mm at 150 mm centres. The stirrups had a yield strength of 382 MPa and a modulus of elasticity of 200 GPa. Ties were also placed in the joints region in accordance with the requirements of AS3600. Additional stirrups and ties and N16 (ϕ = 16 mm); threaded rods were placed near the ends of the beam and column in all specimens to ensure that local failure does not occur at the load and support points respectively. The concrete had a compressive strength around 40, 41, 45, 41, and 37 MPa and a modulus of elasticity around 27.6, 30.1, 29.4, 30.9, and 29.7 GPa for plain (CSM0 and CSC1), retrofitted specimens (RSM1, RSM2 and RSC1) respectively.

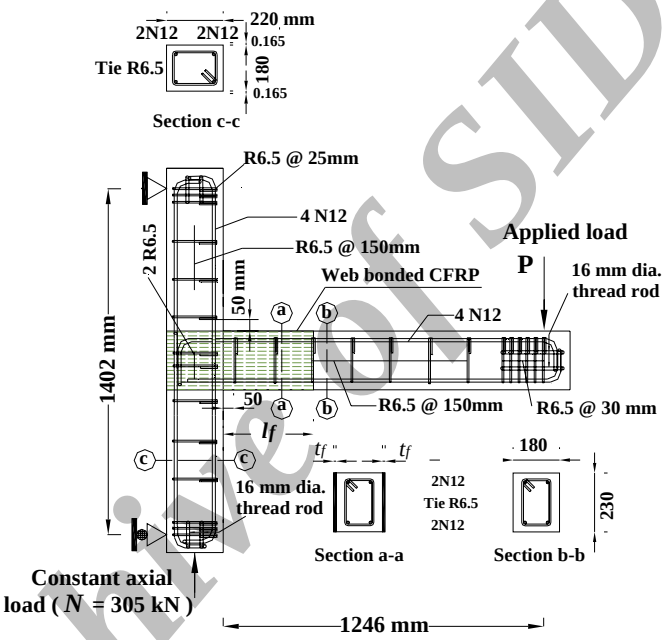

Specimen	l_f (mm)	No. of ply	t_f (mm)
CSM0	-	-	-
RSM1	350	1	0.165
RSM2	200	3	0.495
CSC1	-	-	-
RSC1	200	3	0.495

Figure 7. Specimen's details.

One plain specimen (CSM0) as a control specimen was constructed and was tested under monotonic load to failure. The specimen RSM1 was retrofitted with one ply CFRP sheet at a distance of 350 mm from the column face as is illustrated in Figure 7 and was tested under monotonic loads to failure. Carbon Fibre Reinforced Polymer (CFRP) sheets that were used in all experiments were uni-directional. The beams were not fully wrapped, as it could have been impractical in real situations due to the interface with the concrete slab. Wraps were extended over the joint core area to the back of column in order to minimize the possibility of premature delamination. CFRP was an MBrace Fibre sheeting from MBT [11], which

possesses a tensile strength of about 3900 MPa, a modulus of elasticity of 240GPa and an ultimate tensile elongation of 1.55%. The MBrace Saturant (adhesive) was also used for warping the MBrace sheet using a wet lay up method. The saturant had a minimum tensile strength of 50 MPa and a minimum compressive strength of more than 80 MPa. It's modulus of elasticity was around 3000MPa and it's ultimate elongation around 2.5%. Prior to the application of CFRP web-bonded systems, the surface of the specimen were ground and loose spalled concrete pieces were removed using air jet pressure in order to assure a good bond between CFRP and concrete. It was also buffed clearly using Acetone. A film of primer was applied to fill the cracks and the voids on the damaged areas of the specimens. The primer was allowed to cure for 24 hours after application. The concrete surface was then ground smooth and unidirectional MBrace CF130 sheets (MBT) were applied to a distance of 350 mm within the beam using MBrace Saturant adhesive. The sheets were glued to the web of the beam with the fibres orientation parallel to the beam's longitudinal axis. The second specimen RSM2 (see Figure 7) was retrofitted with three plies of 200 mm CFRP, and was tested under the same loading regime as specimen RSM1.

In order to examine the ability of FRP web-bonded system to retrofit the beam-column joints under cyclic loads, one plain specimen (CSC1) as a control specimen was constructed and tested under cyclic load to failure. The specimen RSC1 was retrofitted with three plies CFRP sheet at a distance of 200 mm from the column face the same as specimen RSM2. This specimen was loaded under the same loading regime as specimen CSC1 to failure.

3.3 Instrumentation and loading

The testing rig was built up into a 3 m by 3 m rigid frame. Figure 8 shows the experimental set-up. The joint was rotated 90° so that the column was parallel and the beam was perpendicular to the ground. The free end of the beam was loaded and the connection between the beam and the actuator was carefully designed in order to ensure that the load could be applied in a push-pull manner. Axial loading of the column was simulated by stretching four high-strength low-elongation steel bars that were placed outside the column by the use of a hydraulic jack while a load cell was utilised to measure the applied load. The column were supported at each end with specially designed supports that ensured their ends were free to rotate but not to translate. This special hinge support was designed to simulate the real performance of the sub-assemblies at the inflection points as well as applying the constant load into the column.

In the first three tests, the loading was applied monotonically by an actuator which was capable of applying cyclic loads for the last two specimens in both load and displacement control regimes. The load was applied first in a load control regime and when the load reached the theoretical first yield, obtained from numerical analysis using ANSYS [12], subsequent tests were then performed using a displacement control regime from the ductility level of one, then 2, then 3 and continued up until failure.

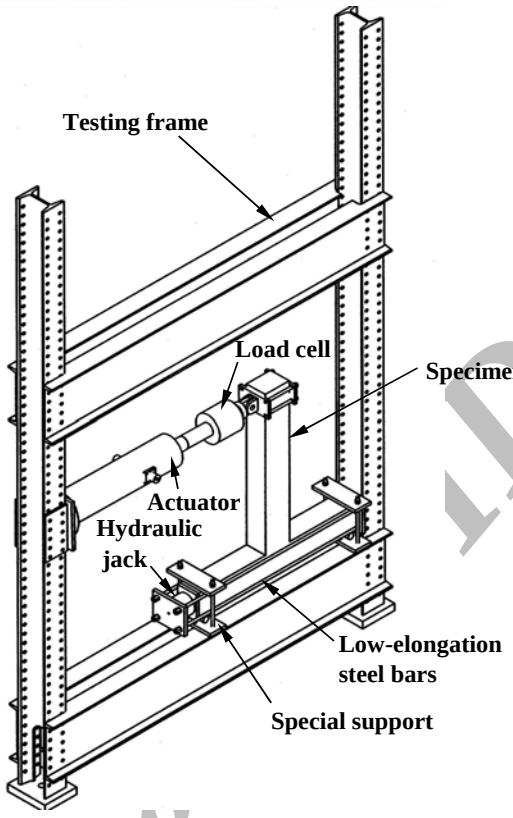

Figure 8. Test set-up

4. EXPERIMENTAL RESULTS AND DISCUSSIONS

The plain control specimen was tested to failure in order to determine it's capacity, flexural stiffness, and failure mode. This specimen was first loaded to initial yield under load control and then to failure under a displacement control regime. When the load corresponding to steel yielding level was reached in the experiments, flexural cracks were developed at the beam-end close to the column face and some flexural cracks were propagated into the joint core. This trend continued up to the end of the test whereas the beam flexural cracks at the column face opened and subsequently the load dropped and the beam collapsed (see Figure 9).

CSM0 RSM1 RSM2

Figure 9. Ultimate failure of specimens CSM0, RSM1 and RSM2.

The retrofitted specimen RSM1 with only one CFRP sheet on the web exhibited a brittle failure. This specimen was tested under a similar loading regime as CSM0. Firstly, flexural cracks in the beam end became more obvious and then the top beam bars started to yield in tension at the column face and some bond deterioration was observed in the main beam bars around the beam end facing the column. At ultimate, concrete crushing occurred at the face of the column, which followed by the beam rotation about the fulcrum, and the rupture of CFRP on the tension side. Subsequently, major cracks were relocated from the cut-off of CFRP to the beam end at the column face. A loud crackling sound was heard at this stage indicating the initiation of concrete crushing and the subsequent rupture of CFRP. No shear cracks were observed in the beam end or within the joint region. Figure 9 shows specimen RSM1 at failure. Specimen RSM2 was tested under the same loading regime as RSM1. Firstly at the displacement ductility of 1, the flexural cracks at the cut-off point of the warp became more obvious and then the top beam bars started to yield near the cut-off point of CFRP. These cracks became wider towards the failure point. Some shear deformations were occurred in the wrapped area. In general, this specimen exhibited a ductile failure. In this specimen, plastic hinges were relocated from the column face to the cut-off point of CFRP as shown in Figure 9.

The beam's tip load versus displacement curves for specimens CSM0, RSM1 and RSM2 are shown in Figure 10. Table 1 shows that the maximum strengths and the estimated ductility of all specimens are tabulated. As is seen the maximum load recorded in these tests were about 24.64, 24.70, and 21.12; for specimens CSM0, RSM1 and RSM2 all in kN respectively. As is shown, the maximum load strength recorded for specimen RSM1 is about that of the plain specimen CSM0 whereas that for specimen RSM2 is only 86% of the maximum strength of plain specimen CSM0. It may relate to the fact that the retrofitting length of this specimen was not sufficient enough to carry loads at the early stages of the test.

The specimen, CSC1, was then subjected to cyclic loading regime. In the seventh cycle at the beam's tip displacement of 47.4 mm, vertical cracks were formed in the joint area close

to the back of column due to the bond deterioration between the column top reinforcements and concrete. Cracking of the concrete due to the flexural deformation of the beam was initiated from the beam end at the column face and grew along the beam length. Some cracks were penetrated into the joint core at beam's tip displacement of 31.6 mm. Crushing and spalling of the concrete occurred in the thirteenth cycle at the tip displacement of 94.8 mm and the corresponding load of 19 kN (pull). This load was the maximum load that the specimen held. The specimen failed soon after when buckling of the beam's top rebar occurred at the column's face. Consequently the load on the specimen started to descend. The final failure pattern is shown in Figure 11. The plastic hinge was formed at the face of the column.

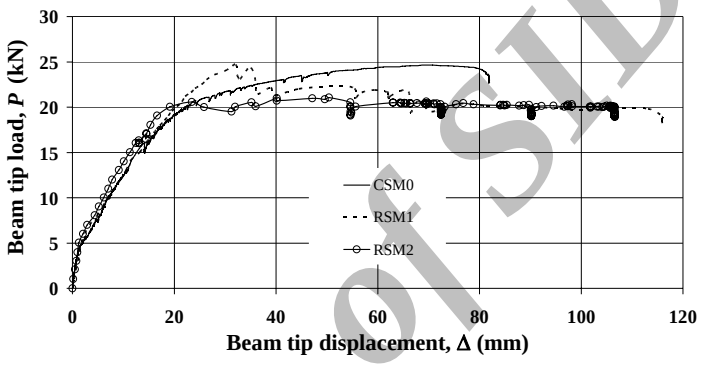

Figure 10. Beam's tip load vr. displacement for specimens, CSM0, RSM1 and RSM2.

Table 1. Summary of the test results

Specimen	Loading type	No. of CFRP plies	CFRP wrapping length mm	Maximum strength kN	Displacement ductility factor	Failure mechanism	Failure location
CSM0	Monotonic	-	-	24.64	5.8	Ductile	Beam end
RSM1	Monotonic	1	350	24.70	-	Sudden	Beam end
RSM2	Monotonic	3	200	21.12	5.7	Ductile	Within the beam
CSC1	Cyclic	-	-	19.52	6.5	Ductile	Beam end
RSC1	Cyclic	3	200	21.32	6	Ductile	Within

the beam

Examining the hysteretic behaviour of the specimen showed severe pinching, stiffness degradation during the test and strength deterioration in the final two cycles followed by spalling of the concrete and the subsequent full buckling of the steel reinforcements at the column face, as shown in Figure 12.

CSC1 RSC1

Figure 11. Failure pattern of specimens CSC1 and RSC1.

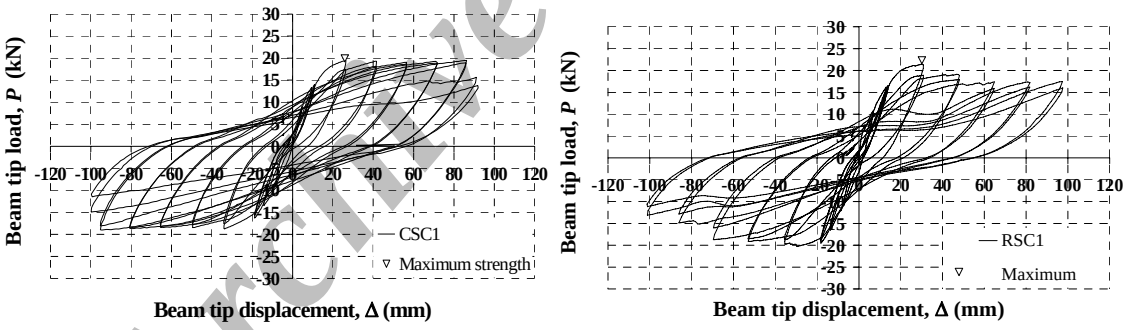

CSC1 RSC1

Figure 12. Load versus displacement for CSC1 and RSC1.

Specimen RSC1 was subjected to the same loading sequence as specimen CSC1. The first crack occurred during the first cycle at the FRP cut-off point. In the second cycle, the specimen was loaded to 16.35 kN (pull and push). This load was again 75% of the theoretical load at which the first yield of steel was expected. The displacement at this load (17.5 mm) was then used as the basis for guessing the displacement at first yield after which the displacement-control regime started. During the first cycle of displacement control, no crack was observed at the column face. In fact all cracks shifted beyond the cut-off of CFRP. The loading continued to the seventh cycle without any debonding of FRP sheets and

only then the first signs of debonding were observed at the mid-height of the beam close to the column face. In the cycles that followed, as the tension in FRP was lost due to de-bonding, steel bars started to carry the developed tensile force. In the ninth cycle, the top steel bars of the beam started to buckle. This buckling occurred around 150mm away from the column face. The position of buckled steel rebar can arguably be thought of as the centre of plastic hinge. Assuming this, FRPs have been able to shift the location of plastic hinge 150mm away from the column face. This is about 65% of the section depth and three quarter of the length of FRP coverage. As for the load, the specimen reached a maximum load of 21.33 kN (pull) and 20.16kN (push) in fifth cycle and then experienced a decreasing trend to a load of 19 KN in the seventh cycle. The strength of the specimen was almost maintained up to failure. The final failure conditions before and after removing the CFRP from concrete surface are shown in Figure 11. Examining the hysteretic loops of the specimen (Figure 12) shows that the energy absorbing capacity is maintained as the maximum loads hold to a healthy plateau up to the end. No considerable pinching, stiffness degradation or strength deterioration was observed in the final two cycles as was the case for the plain RC specimen. This obviously is a result of plastic hinge region being confined by the FRP sheet to some extent.

Beam CSC1 rotated at the column face while beam RSC1 about an axis located almost 150mm away from the column face within the beam. Elastic movements away from the plastic hinge were small compared to the plastic deformations and therefore the final deformed shape was basically a function of plastic hinge rotations.

Another evidence indicating the satisfactory behaviour of the retrofitted specimens is their displacements ductility. The displacement ductility factor required of typical structures may vary between 1 for elastically responding structures to 6 for ductile structures. For structures in which ductility is controlled by flexural plastic hinging of members, for instance the retrofitted specimens RSM1 and RSM2, the displacement ductility is limited by the special manner of failure. In specimen RSM1 in which the beam end was retrofitted only with one ply of CFRP sheet, the load capacity of the specimen was improved well, although the post peak reduction was not smooth as CFRP ruptured at the column face and the specimen failed by concrete crushing that followed that rupture (see Figures 9, 10). This particular type of failure does not allow for adequate ductility and as such the ductility factor cannot be determined. In contrast, as is seen in Figure 9, specimen RSM2 did not exhibit a sudden failure and the CFRP warp remained intact to failure. The beam deformed significantly at the cut-off point of the wrap, and although some shear deformation occurred at the beam end, it did not affect the ductility of the specimen. Table 1 contains the displacement ductility factor of specimen RSM2. The ductility factor for the specimen RSM2 is equal to 5.7 which is about that of the plain specimen CSM0.

Figures 11 and 12 show the failure mechanisms and beam-tip load verus displacements of specimens CSC1 and RSC1 respectively and Table 1 contains the estimated displacement ductility factor for these specimens. As is seen, an almost similar displacement ductility were calculated for these specimens whereas the failure of specimen RSC1 is located further from the beam end and joint core indicating that the plastic hinge in this specimen is relocated from the joint core toward the beam under cyclic loading regime and therefore the performance of the frame is converted into a ductile manner.

CONCLUSIONS

The test results reported herein have led to the following conclusions concerning the plastic hinge location.

1. Web-bonded CFRP-retrofitting technique can be used to relocate the beam plastic hinging zone away from the column face in RC ordinary moment resisting frames.
2. Use of over-designed FRP-retrofitting increases the strength of the beam end so that the beam sections adjacent to the column face remain essentially elastic.
3. Use of CFRP transverse wrap is recommended in order to confine the retrofitted areas and reduce the shear deformation.
4. In the aforementioned tests, the retrofitted specimens' flexural yielding occurred at the expected critical sections. Inelastic deformations occurred about 150 mm away from the column, indicating that the relocation has been achieved.

With regard to the cyclic behaviour:

The CFRP-retrofitted specimen developed flexural yielding at the expected critical section.

1. The proposed web-bonded FRP allowed the energy dissipation in the hysteretic behaviour to occur in a ductile manner.
2. A retrofitting length at least 1.3 times of the beam height is recommended in order to fully relocate the plastic hinge away from the column in moment resisting frames subjected to cyclic loads in order to guarantee a ductile manner after retrofitting.

Acknowledgments: Authors would like to express their thanks to MBT Australia for making carbon fibres and other materials available to them at a subsidised rate. The first author is supported by a combined IPRS-UQIPRS scholarship from the Australian Federal government and the University of Queensland for the duration of his PhD. The support that has enabled him to perform the current research is gratefully acknowledged.

REFERENCES

1. Abdel-Fattah, B. and Wight, J.K., Studies of Moving Beam Plastic Hinging Zones for Earthquake-Resistant Design of R/C Buildings, ACI Structure Journal, No. 1, **84**(1987) 31-39.
2. Joh, O., Goto, Y., and Shibata, T., Influence of Transverse Joint and Beam Reinforcement and Relocation of Plastic Hinge Regions on Beam-Column Joint Stiffness Deterioration, Design of Beam-Column Joint for Seismic Resistance, J. Jirsa, ed., American Concrete Institute, Farmington Hills, Mich., 1991, pp. 187-223.
3. Paulay, T., and Priestley, M.J.N., Seismic Design of Reinforced Concrete and Masonry Buildings, John Wiley and Sons, INC, 1992.
4. Mahini, S.S., Ronagh, H.R. and Dux P.F., Flexural Repair of RC Exterior Beam-Column Joints Using CFRP Sheet, Proceeding of The Second International Conference on FRP Composites in Civil Engineering, Adelaide, Australia, 8-10 December, 2004,

pp. 653-658.
5. Mahini, S.S., Ronagh, H.R. and Smith S.T., CFRP-retrofitted RC Exterior Beam-Column Connections under Cyclic Loads, Proceeding of The Second International Conference on FRP Composites in Civil Engineering, Adelaide, Australia, 8-10 December (2004) 647-652.
6. ACI-ASCE Committee 352, Recommendations for Design of Beam-Column Joints in Monolithic Reinforced Concrete Structures, *ACI Journal*, No. 3, **82**(1985) 266-283.
7. ABA, Iranian Concrete Code, 2005.
8. AS3600, Concrete Structures, Standards Australia, 2001.
9. ACI318, Building Code Requirements for Structural Concrete, American Concrete Institute, 2002.
10. Noor, F. A., and Boswell, L. F., Small Scale Modelling of Concrete Structures, Elsevier Science Pub. Co, 1992.
11. MBT, MBrace, Composite Strengthening System, Master Builders Technologies: (MBT Australia) Pty Ltd., 2002.
12. ANSYS Manual Set., ANSYS, Inc.: Canonsburg, PA 15317, USA, 2003.